RSC Pharmaceutics

Accepted Manuscript

This article can be cited before page numbers have been issued, to do this please use: M. Baghbanbashi, R. Burnett, D. Gooden, F. Vago, H. F. Staats, B. T. Johnson-Weaver and K. Ristroph, *RSC Pharm.*, 2026, DOI: 10.1039/D6PM00082G.

View Article Online
DOI: 10.1039/D6PM00082G

Hapten-conjugated polymeric nanocarriers produced by Flash NanoPrecipitation induce small molecule-specific antibodies *in vivo*

*Mojhdeh Baghbanbashi[1], Ryan Burnett[2], David M. Gooden[3], Frank S. Vago[4], Herman F. Staats[2], Brandi Johnson-Weaver[2], Kurt Ristroph[1,5]**

1. Department of Agricultural and Biological Engineering, Purdue University, West Lafayette, Indiana, 47907, United States

2. Department of Pathology, Duke University School of Medicine, Durham, North Carolina 27708, United States

3. Small Molecule Synthesis Facility, Duke University, Durham, North Carolina 27708, United States

4. Bindley Bioscience Center, Purdue University, West Lafayette, Indiana, 47907, United States

5. Davidson School of Chemical Engineering (by courtesy), Purdue University, West Lafayette, Indiana, 47907, United States

* - ristroph@purdue.edu

ABSTRACT

Vaccines that induce antibodies specific against small molecules are desirable for a range of applications, including as a tool against the opioid epidemic. Many small molecules are not immunogenic due to their low molecular weight, but can be conjugated to larger carriers such as immunogenic proteins to induce an immune response. Achieving a high hapten surface density and hapten-specific antibody induction remains a challenge. In this study, we used Flash NanoPrecipitation (FNP) to form polymeric nanocarriers with a surface layer of poly(caprolactone)-b-poly(ethylene glycol)-hapten, using trinitrophenol (TNP) as a model hapten.

View Article Online
DOI: 10.1039/D6PM00082G

Different levels of TNP surface coverage were tested: 0%, 1%, 10%, 50%, and 100% of polymer chains terminated with TNP. NCs were administered by intramuscular immunization to BALB/c mice along with antigenic protein ovalbumin, either free in solution or encapsulated into the cores of the NCs. At fixed TNP mass per dose, NCs induced serum TNP-specific IgG antibodies, with higher titers induced by NCs with a higher percentage of surface chains terminated with TNP. This demonstrates proof of principle for the use of NCs made by FNP as hapten carriers that can be rapidly developed, as an alternative to hapten-protein conjugates that rely more heavily on protein and hapten chemistry.

View Article Online
DOI: 10.1039/D6PM00082G

INTRODUCTION

Opioid abuse disorder (OUD) is a public health crisis that leads to addiction, overdose death, and social impact on more than 35 million people worldwide, including over 2.1 million in the United States. The reported overdose related deaths in the United States have increased to 81,806 in 2022 [1–5]. One approach to combating opioid overdoses is the use of medications designed to reduce the effects of opioids, but overdose rates remain high due to limited accessibility, inconsistent treatment recommendations, and misuse of these medications [2,6,7].

Vaccination is another approach to mitigating the biological effects of opioids and reducing overdose incidence which has gained significant attention in research. Opioid molecules are not inherently immunogenic due to their low molecular weight, but they can be used as haptens by chemically conjugation to the surface of a carrier, that induce an immune response [8]. Vaccines that produce high titers of high-affinity antibodies against an opioid should be able to bind that opioid in circulation, prohibiting it from entering the brain. Several studies suggest the hapten structure[9], hapten density[10], carrier molecule[11], and adjuvant[12,13] are all important variables that influence the efficacy of opioid vaccines. The carrier used for hapten conjugation should possess specific properties including proteinaceous character to provide T cell help, a high opioid surface density, and proper formulation to facilitate administration[8].

Proteins have often been used as carrier molecules for opioid haptens. The carriers used in candidate opioid vaccines provide $CD4^+$ T cell help that enhances the host antibody response to the opioid and may improve the ability of the anti-opioid antibody to subsequently block the biological activity of the opioid when used as a drug of abuse[14]. Traditional protein carriers for conjugate vaccines include tetanus toxoid (TT) and cross-reactive material 197 (CRM197), a

View Article Online
DOI: 10.1039/D6PM00082G

nontoxic mutant of diphtheria toxin, and keyhole limpet hemocyanin (KLH)[10,12,14–17]. A drawback of using proteins as carriers is that protein-hapten systems have been reported to induce antibodies that are primarily specific to the carrier protein itself, rather than the hapten[18].

One study reported lipid–polylactic acid (PLA) and lipid–poly(lactic-co-glycolic acid) (PLGA) nanoparticles used as a carrier [19]; in that work, the hapten was conjugated on the surface of the lipid-PLGA or lipid-PLA nanoparticles following formulation, which adds complexity to the overall formulation process[19]. Another pair of studies evaluated a bacteriophage Qβ virus-like particle (VLP), which has innate immunogenicity due to foreign proteins in the Qβ VLP, as a nanoparticle carrier for a nicotine hapten[20,21]. Pre-existing immunity to carrier proteins or nanoparticles, such as Qβ VLPs, may reduce the immunogenicity of other vaccines utilizing the same carrier and also impact the efficacy of opioid conjugate vaccines, if repeated doses are required to induce and maintain high-titer anti-opioid antibodies[21]. Many candidate vaccines for drugs of abuse are immunogenic and they induce drug-specific antibodies, but the anti-drug antibodies they induce do not effectively block the biological activity of the drugs *in vivo* and only a fraction of the induced antibodies may exhibit high affinity for the opioid[14]. Consequently, there is significant potential for improvement in the current vaccines targeting opioids.

As represented in Figure 1, a scalable nanoparticle formulation platform, Flash NanoPrecipitation (FNP)[22–25], is employed in this work for the first time to develop polymeric haptenated nanocarriers for small molecule vaccines. A representative small molecule hapten, trinitrophenol (TNP), is chemically conjugated to an amphiphilic diblock copolymer, poly(caprolactone)-b-poly(ethylene glycol) (PCL-*b*-PEG). TNP was selected as a well-established

View Article Online
DOI: 10.1039/D6PM00082G

model hapten that enables controlled and quantitative evaluation of hapten-specific immune responses[26]. The modular nature of the nanocarrier platform allows straightforward substitution of TNP with structurally relevant opioid haptens in future work. The resulting PCL-*b*-PEG-TNP is then used in the organic feed stream to FNP as the amphiphilic surface stabilizer on the nanocarriers (NCs). NCs are prepared with and without ovalbumin (OVA), a $CD4^+$ antigen protein encapsulated into the core, to assess the effect of dosing TNP-decorated NCs with free antigen versus TNP-decorated NCs containing encapsulated protein antigen. OVA contains several T-helper epitopes, including: OVA323-339, OVA55-62, OVA176-183, and OVA257-264[27,28] and we previously reported encapsulating it with FNP[29].

The effect of hapten surface density is also explored. Polymeric NCs produced via FNP have a core-shell structure with a shell consisting of a dense layer of surface polymer, up to two polymer chains per square nanometer[23]. Therefore, up to approximately 60,000 haptens can be installed on a nanocarrier 100 nm in diameter if 100% of surface polymer chains were terminated with TNP, in contrast to the surface density of 10-15 haptens per protein carrier reported in the literature. We also hypothesized that positioning of the hapten at the end of a 5kDa PEG chain to provide physical separation from the ovalbumin may provide a higher hapten-specific response and lower ovalbumin-specific response than in protein-hapten conjugates[19]. By introducing a mixture of PCL-*b*-PEG-TNP and non-haptenated diblock copolymer into the FNP process, the percentage of surface chains terminated in the hapten can easily be tuned from 0% to 100%, allowing rapid single-step preparation of NCs with a variety of hapten surface densities.

View Article Online
DOI: 10.1039/D6PM00082G

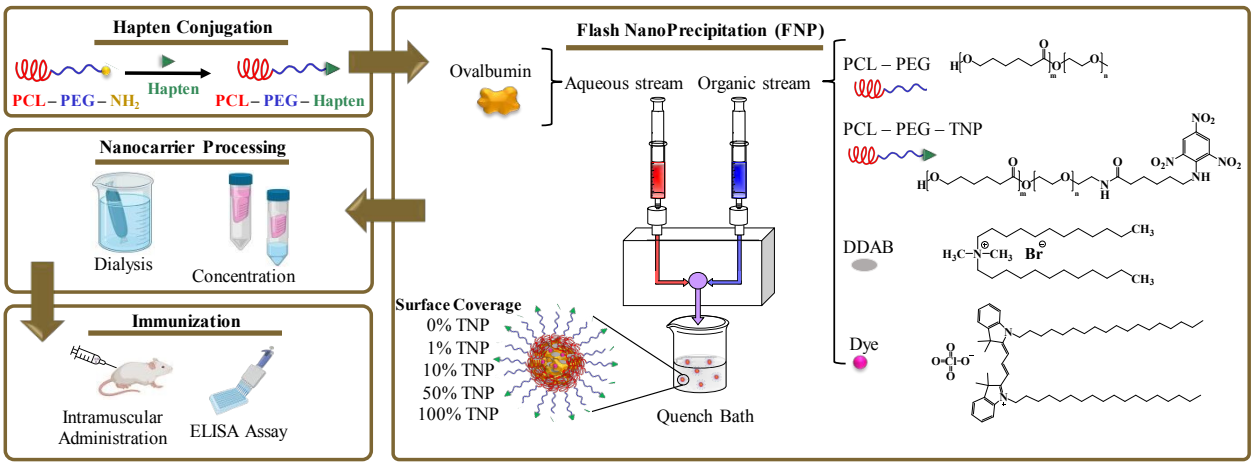

Figure 1. Schematic representation of the experimental procedure implemented in this study.

MATERIALS

Vitamin E acetate: DL-α-Tocopherol acetate (VitEAc) (HPLC,≥96%), dimethyl ditetradecyl ammonium bromide (DDAB) (≥97.0%), 1,1′-dioctadecyl-3,3,3′,3′-tetramethylindocarbocyanine perchlorate (DiI) (97%), 1,4,8,11,15,18,22,25-octabutoxy-29H,31H-phthalocyanine (762 dye) were purchased from Sigma Aldrich (St. Louis, MO, USA). Poly(styrene)-block-poly(ethylene glycol) ($PS_{1.6K}$-b-$PEG_{5.0k}$) and poly (ε-caprolactone)-block- poly(ethylene glycol) ($PCL_{2.9k}$ – PEG_{5k}) were obtained from Polymer Source Inc. (Montreal, Canada). Tetrahydrofuran (THF, HPLC, 99.8%) and nuclease-free water were obtained from Thermo Fisher Scientific (Waltham, MA, USA). EndoFit OVA protein (OVA) and OVA-TNP were obtained from Invivogen (Cat# vac-pova, San Diego, CA, USA) and Biosearch Technology (Cat# T-5051-10, Hoddesdon, UK), respectively. Monophosphoryl lipid A (MPL) was purchased from Enzo Life Sciences (Cat# ALX-581-202-L001, Farmingdale, NY, USA). 2,4,6-trinitrophenol (TNP) was purchased from Santa Cruz Biotechnology (TNP-e-Aminocaproyl-OSu, Cat. # sc-396492, Dallas, TX)

View Article Online
DOI: 10.1039/D6PM00082G

Poly(caprolactone)$_{5k}$-b-poly(ethylene glycol)$_{5k}$-amine (PCL-PEG-NH_2·HCl) was purchased from Nanosoft Polymers (Winston-Salem, NC, USA).

METHODS

PCL-b-PEG-TNP conjugation

The schematic representation of conjugation of TNP to PCL-b-PEG-NH_2 is shown in Scheme 1. The PCL-b-PEG-NH_2. HCl polymer (1 g) and the TNP-ε-aminocaproyl-NHS ester (480 mg, 1.3 mmol) were suspended in CH_2Cl_2 (20 mL). Neat N,N-diisopropylethylamine (DIEA, 300 uL, 1.7 mmol) was added in one portion and the mixture was stirred overnight (16h) at room temperature then concentrated to dryness under reduced pressure. Purification by flash column chromatography (Redisep Rf, SiO_2, 12g, 100% CH_2Cl_2 → 5% MeOH in CH_2Cl_2) gave the conjugate as an orange glassy solid (120 mg).

^{1}H NMR (400 MHz, $CDCl_3$): δ_H (ppm) 1.24 (4H, s, C-CH_2-C), 1.37 (44H, m, J = 4.39 Hz, (-OOC-C-C-CH_2-)$_{22}$), 1.64 (88H, m, J = 3.72 Hz, (-OOC-C-CH_2-C-CH_2-)$_{22}$), 2.20 (2H, t, J = 7.34 Hz, -OC-CH_2-C-C-), 2.29 (44H, t, J = 7.52 Hz, (-OOC-CH_2-)$_{22}$), 3.44 (4H, m, J = 4.50 Hz, -PEG-C-CH_2-N, C-CH_2-TNP-), 3.63 (464H, s, PEG), 3.80 (4H, t, J = 4.96 Hz, PCL-C-CH_2-O, PEG-CH_2-C-N-), 4.05 (44H, t, J = 6.66 Hz, (-CH_2-OOC-)$_{22}$), 4.21 (2H, t, J = 4.96 Hz, PCL-CH_2-C-), 9.02 (2H, s, H-TNP).

View Article Online
DOI: 10.1039/D6PM00082G

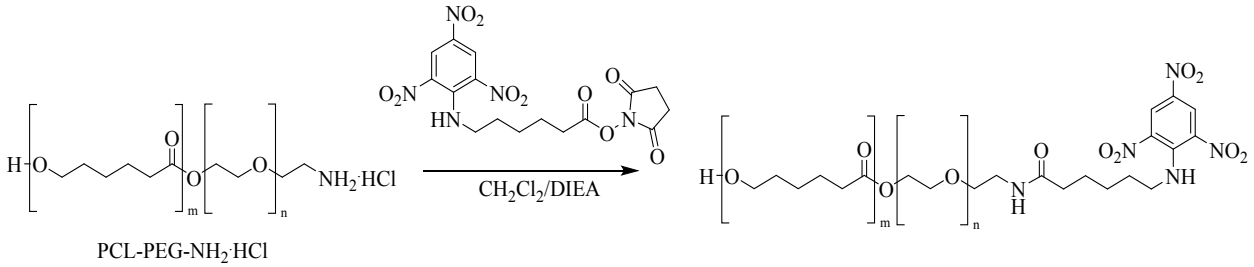

Scheme 1. Synthesis of PCL-b-PEG-TNP

TNP nanocarrier formulations

TNP nanocarriers for co-administration with OVA: Polymeric nanocarriers with various TNP surface coverages (0, 10, and 100% of surface polymers terminated in TNP) and a non-immunogenic core (vitamin E acetate) were prepared by FNP using a confined impinging jets mixer (CIJ) as reported previously.[26,27] In brief, 1 mL of a THF solution containing 5 mg/mL of stabilizer (PS-*b*-PEG / PCL-*b*-PEG-TNP, varying based on the TNP coverage percentage), 4.9 mg/mL VitEAc, and 0.1 mg/mL 762 dye, and 1 mL of RNase free water, were each loaded into a 1mL Luer-slip syringe and attached to the mixer. The syringes were rapidly injected into the CIJ and the resulting effluent was collected in 8 mL DI water, then dialyzed against RNase free water to remove THF.

TNP nanocarriers encapsulating OVA: OVA as a T helper protein was encapsulated in the nanocarriers with various hapten surface coverages (0, 1, 10, 50, and 100% of surface polymer chains terminated in TNP). Hydrophobic ion pairing was used in conjunction with FNP to encapsulate the water-soluble OVA, as reported previously.[29] The OVA:counterion (DDAB) molar ratio was 1:96 such that 2 DDAB cations were present per each anionic group of OVA[29]. The organic stream consisted of 5 mg/mL stabilizer (PCL-*b*-PEG / PCL-*b*-PEG-TNP with various mass

View Article Online
DOI: 10.1039/D6PM00082G

concentrations to obtain desired hapten surface coverage), 5.53 mg/mL DDAB as the counterion, and 0.21 mg/mL DiI in THF. Ovalbumin at 5 mg/mL in RNase free water was used as the antisolvent stream. 0.5 mL of each stream were mixed using a CIJ and collected in 4 mL of RNase free water. The obtained formulations were dialyzed against RNase free water to remove the organic solvent.

Characterization

Nanocarrier size, polydispersity, and zeta potential were measured using a Zetasizer Pro (Malvern Instrument Ltd.). Samples were diluted 10-fold in Milli-Q water for size and polydispersity measurements using dynamic light scattering at a 173˚ backscatter and 25˚C. To measure the zeta potential of NCs, samples were diluted 10-fold in 20 mM NaCl aqueous solution.

Nanocarrier concentration

The nanocarriers containing VitEAc in the core were concentrated prior to use to normalize the mass of TNP in each dose. The 0% and 100% TNP-terminated formulations were concentrated 2-fold, and the 10% TNP formulation was concentrated 20-fold. The concentration was carried out by centrifugal ultrafiltration of nanocarrier solution using 10kDa Amicon filters (Sigma Aldrich) at 5000g for 20min. In order to freeze and store these NCs, 6kDa PEG as a cryoprotectant was added to the nanocarriers solution to a final PEG:NC mass ratio of 5:1. The nanocarriers containing OVA were centrifuged in the 100kDa Amicon filters at 7000 rcf for 4 min to concentrate them 6-fold prior to dosing into animals.

Cryo Transmission Electron Microscopy (cryo-TEM)

View Article Online
DOI: 10.1039/D6PM00082G

To prepare grid specimens for cryo-TEM, QUANTIFOIL® R 1.2/1.3 300 mesh Cu grids (Quantifoil Micro Tools GmbH) were first glow-discharged in a PELCO easiGlow™ system (Ted Pella, Inc.) for 60 seconds at 25 mA. A 3 μL aliquot of concentrated nanocarriers was applied to the grids, blotted for 5 seconds with a blot force setting of 3 and immediately plunged frozen into liquid ethane using a Vitrobot Mark IV System (Thermo Fisher Scientific). Grid specimens were imaged in a Thermo Fisher Scientific Talos F200C transmission electron microscope operated at 200 kV in low-dose mode. Images were captured with a Ceta 4k × 4k CMOS camera (Thermo Fisher Scientific) at a nominal magnification of 33,000X, a defocus around -5 μm and a total electron dose of around 50 e^-/A^2.

Nuclear Magnetic Resonance (NMR) Spectroscopy

The ^1H NMR spectrum was recorded at room temperature on a Bruker AVANCE III HD 400 MHz spectrometer, equipped with a 2-channel Nanobay console and a 5mm BBFO Z-gradient SmartProbe. Spectral processing and analysis were performed using Bruker TopSpin software (version 4.3.0).

Nanocarrier immunogenicity *in vivo*

The immunogenicity of the nanocarriers was assessed after intramuscular immunization in BALB/c mice. Young adult female BALB/c mice (8-10-week-old) were intramuscularly immunized with an OVA-TNP conjugate vaccine positive control, TNP-decorated FNP NCs not containing OVA (0, 10, 100% of polymer chains terminated with TNP) co-administered with dissolved OVA, or TNP-decorated FNP NCs (0%, 1%, 10%, 50%, or 100% of surface chains terminated with TNP) containing encapsulated OVA. Each 50 μL vaccine dose was normalized to

View Article Online
DOI: 10.1039/D6PM00082G

contain 10 μg of OVA and 10 μg of MPL as an adjuvant. Mice were immunized on experimental days 0 and 14. Day 0 immunizations were performed in the right hind leg, and day 14 was administered in the left hind leg. Serum was collected via submandibular vein punctures on day 28 or 35. The serum samples were measured for vaccine-induced OVA-TNP-, OVA-, and TNP-specific antibodies by enzyme-linked immunosorbent assay (ELISA).

Enzyme-Linked Immunosorbent Assay

ELISA was performed as previously described[28] except that ELISA plates were coated with OVA-TNP, OVA or TNP-BSA at 2 μg/ml and incubated overnight at 4^0C. Serum samples from immunized mice or an unimmunized, naïve mouse as a reference control were serially diluted 2-fold beginning at an initial dilution of 1:32. Diluted serum samples were incubated on antigen-coated plates overnight at 4^0C. After washing, the ELISA plates were incubated at room temperature for 2 hours with an alkaline phosphatase conjugated goat anti-mouse IgG secondary antibody diluted 1:8000. The fluorescent Attophos substrate system (Promega) was used to develop the ELISA plates. End-point titers were defined as the last sample dilution that provided a relative light unit (RLU) signal that was 3-fold greater than the naïve reference sample at the same sample dilution.

Statistical Analysis

GraphPad PRISM (version 10, Boston, MA) was used to perform all statistical analyses. The Log2 end-point titers were used to compare antigen-specific serum IgG responses using a nonparametric Kruskal-Wallis test with a Dunn's multiple comparisons post-test compared to the indicated control group. A p-value of < 0.05 was considered statistically significant.

View Article Online
DOI: 10.1039/D6PM00082G

RESULTS AND DISCUSSIONS

PCL-b-PEG-TNP conjugation

After conjugating the hapten to PCL-PEG-NH_2, the reaction solution was purified using flash column chromatography which removes excess hapten and DIEA. The final product was studied by ^{1}H NMR characterization. As shown in the ^{1}H NMR spectrum of PCL-PEG-TNP (Figure *2*), the presence of the peak of TNP functional group at 9.02 ppm and the linker group at 1.24, 2.20, and 3.45 confirms the successful conjugation. The extent of TNP conjugation to PCL-b-PEG-NH_2 was determined by ^{1}H NMR spectroscopy. The starting polymer was $PCL_{2.9kDa}$–PEG_{5kDa}–NH_2. A 5 kDa PEG block corresponds to a degree of polymerization (DP) of approximately 113.63 ethylene glycol units, giving rise to a characteristic PEG methylene resonance at 3.63 ppm (–CH_2CH_2O–), corresponding to 4 protons per repeating unit (total theoretical integration = 454 protons). Upon conjugation with TNP, the aromatic proton signal of the TNP group at 9.02 ppm was used as an internal reference and was calibrated to 2 protons. The integration of the PEG peak at 3.63 ppm was consistent with the theoretical value expected for the PEG block (~454 protons). This agreement indicates essentially quantitative end-group conversion, corresponding to ~100% conjugation of TNP to PCL-b-PEG-NH_2 within the accuracy of ^{1}H NMR analysis.

View Article Online
DOI: 10.1039/D6PM00082G

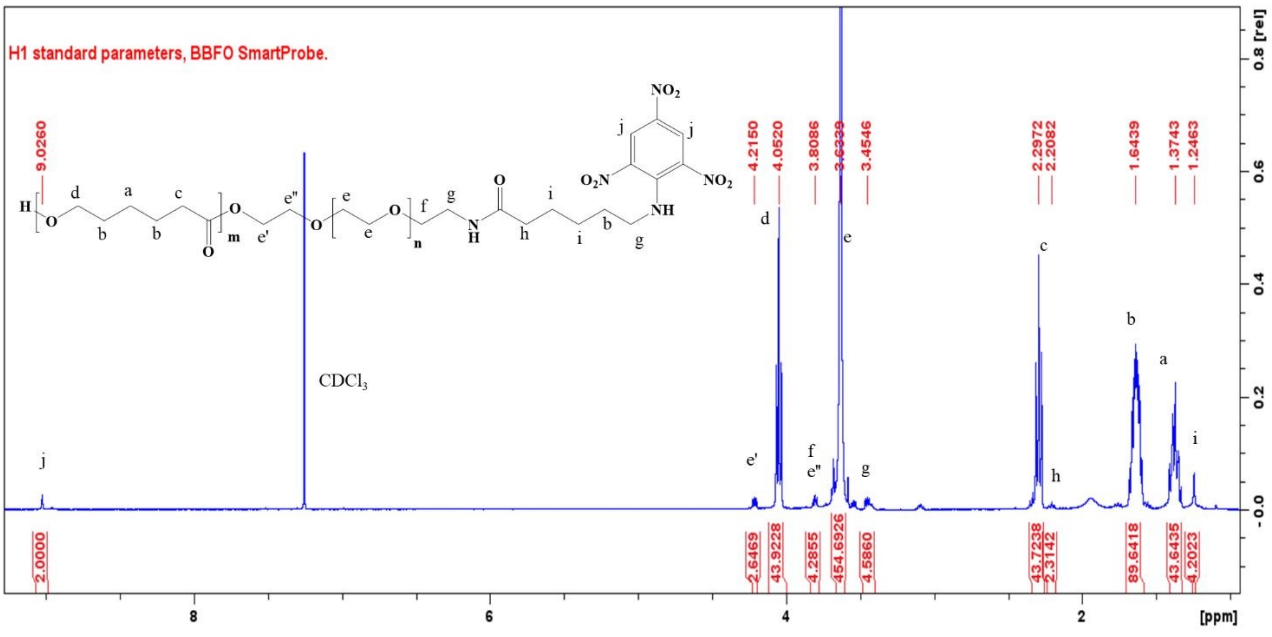

Figure 2. ^{1}H NMR spectra ($CDCl_3$) of PCL-PEG-TNP

Nanocarrier formation and characterization

Nanocarriers were prepared using FNP in a CIJ mixer, a turbulent mixing device that enables rapid and reproducible nanoparticle formation[24,30]. In this process, depending on the formulation VitEAc or counterion (DDAB), and amphiphilic diblock copolymers (PCL-*b*-PEG or PCL-*b*-PEG-TNP) were dissolved in THF, a solvent for all organic components, and rapidly mixed with water as a miscible antisolvent. THF was selected due to the complete solubility of the hydrophobic core materials and copolymers, while water serves as an effective antisolvent for VitEAc, DDAB-OVA complex, and the hydrophobic PCL block. Rapid turbulent mixing in the CIJ induces simultaneous precipitation of the hydrophobic core material and the hydrophobic block of the copolymer, forming NCs that are sterically stabilized by the hydrophilic PEG corona[24]. It is shown that when the inlet syringes (Figure 1) are rapidly pushed with hand, the CIJ mixer operates in the turbulent regime where particle size becomes insensitive to small variations in inlet velocity once a critical

View Article Online
DOI: 10.1039/D6PM00082G

Reynolds number is exceeded, providing robustness to batch-to-batch variations in syringe-driven flow rates[25,31,32].

TNP-decorated nanocarriers not containing OVA: NCs with different amounts of TNP on the surface and VitEAc in the core were formed in the range of 58.9 – 68.0 nm with a narrow PDI of 0.09-0.16, indicating uniform particle populations (Figure 3A). Increasing TNP surface coverage did not substantially change NC size or PDI, demonstrating that surface functionalization was achieved without compromising colloidal stability. Following dialysis and concentration, NC size and PDI were unchanged and after freeze/thaw the size and PDI remained within 16% of the initial values, further confirming structural stability during processing (Figure 3A). All formulations exhibited neutral to slightly negative zeta potentials (Figure 3B) with unchanged surface charge with increasing TNP density from 10% to 100%. This indicates that the PEG corona shields the surface of the NCs and the TNP group present at the distal end of PEG chains is not strongly ionized under the formulation conditions. VitEAc was encapsulated as a hydrophobic core material that does not contribute biological activity in this study but serves as a bulking agent to maintain consistent core composition and NC size across formulations. This design ensures that observed differences in immunological outcomes can be attributed primarily to differences in TNP surface density rather than variations in NC size, dispersity, or core composition. These formulations were subsequently evaluated *in vivo* via co-administration with free OVA to assess the effect of hapten surface density on immune response.

View Article Online
DOI: 10.1039/D6PM00082G

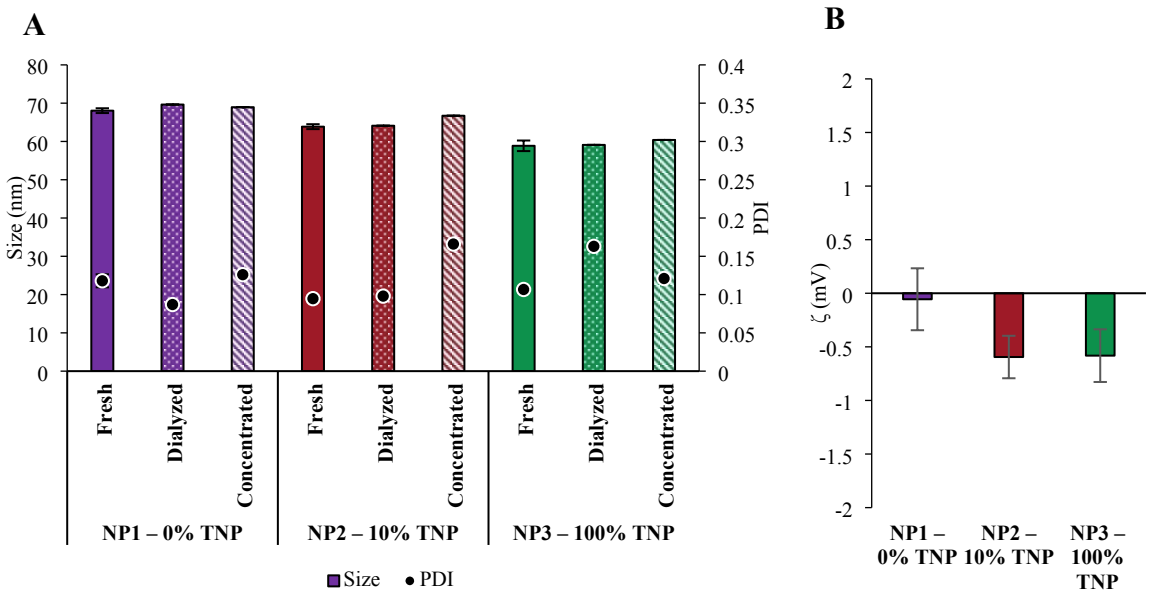

Figure 3. A) Size, PDI, and B) zeta potential (ζ) of TNP nanocarriers encapsulating VitEAc with different TNP surface coverages. Error bars represent the standard deviation of three different measurements.

TNP-decorated nanocarriers containing OVA: Since OVA is hydrophilic and soluble in water (50 mg/mL), in order to encapsulate it in nanocarriers by FNP, hydrophobic ion pairing with a hydrophobic counterion was used to form an ionic complex that precipitates in water to form the nanocarrier core. A previously reported formulation employing DDAB as a cationic hydrophobic counterion was reproduced[29]. In this work, a combination of PCL-b-PEG-TNP and PCL-b-PEG was utilized as the surface stabilizer, in contrast to the original study, which used only PCL-b-PEG. NCs 131-147nm in diameter with a narrow PDI of 0.18-0.24 and a neutral zeta potential were formed. The difference in zeta potential between VitEAc-loaded and OVA-loaded NCs arises from the formulation strategy used for protein encapsulation. OVA carries approximately 48 negatively charged residues[29]. To facilitate electrostatic complexation and encapsulation, an excess

View Article Online
DOI: 10.1039/D6PM00082G

of the cationic counterion DDAB was used at an OVA:DDAB molar ratio of 1:96, corresponding to approximately two DDAB molecules per anionic group on OVA. The presence of excess cationic counterion in the formulation results in a net positive surface charge, leading to a slightly more positive zeta potential for OVA-loaded NCs compared to VitEAc-loaded NCs. NC size was constant after dialysis and 6-fold concentration and did not change over at least 15 days (Figure 4). The encapsulation efficiency of OVA was previously measured and reported at ~85%[29].

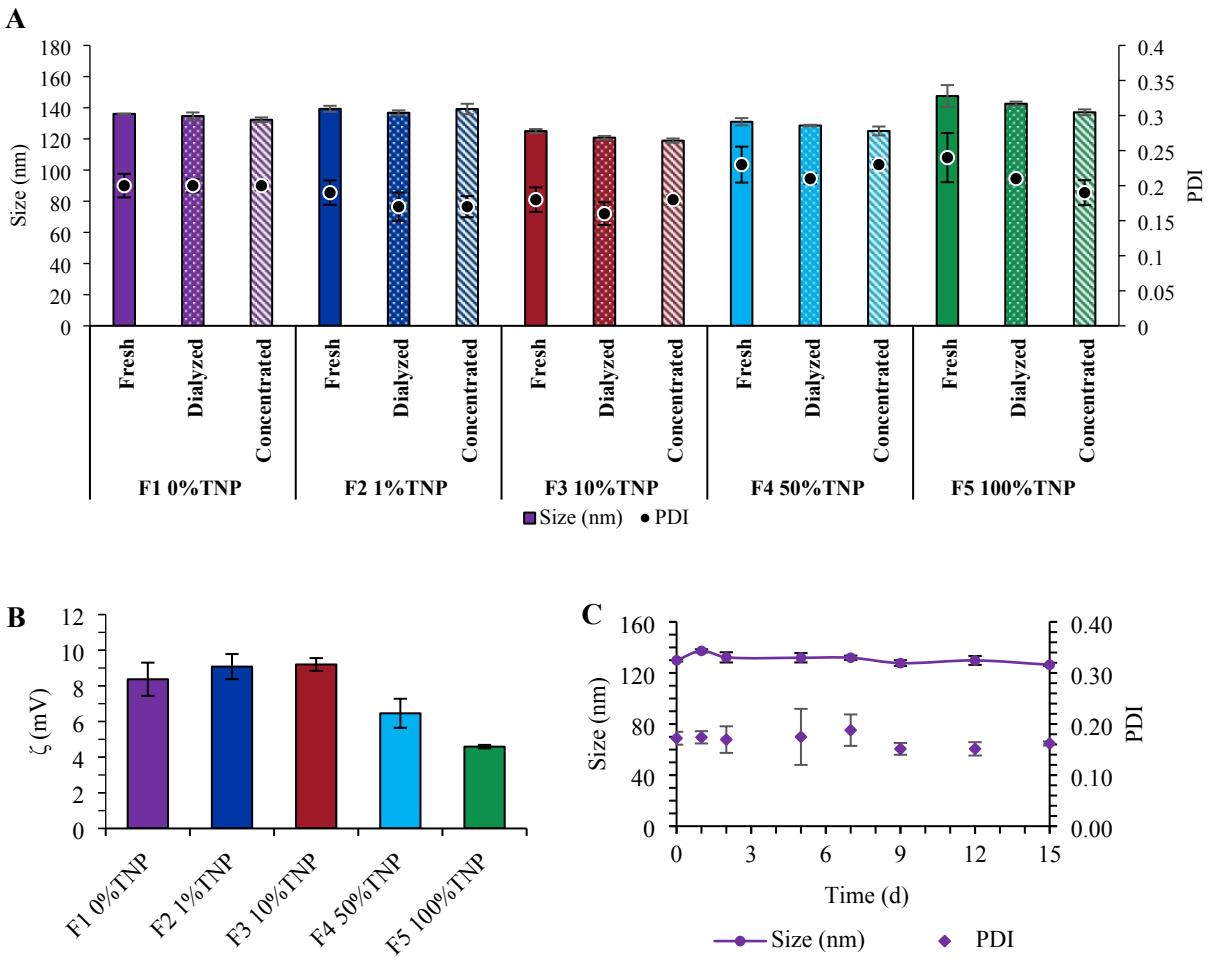

Figure 4. (A) Size, PDI, and (B) zeta potential (ζ) of TNP nanocarriers encapsulating OVA with different TNP surface coverages which were used in the liquid state. (C) Size over time of

View Article Online
DOI: 10.1039/D6PM00082G

nanocarriers encapsulating OVA with 0% TNP surface coverage. Error bars represent the standard deviation of three different measurements.

The TNP-decorated nanocarriers encapsulating VitEAc or OVA were characterized by cryo-TEM, and representative images are shown in Figure 5A and B, respectively. The nanoparticles exhibited a predominantly spherical morphology with well-defined structures and a relatively uniform size distribution, confirming the successful formation of the nanocarriers.

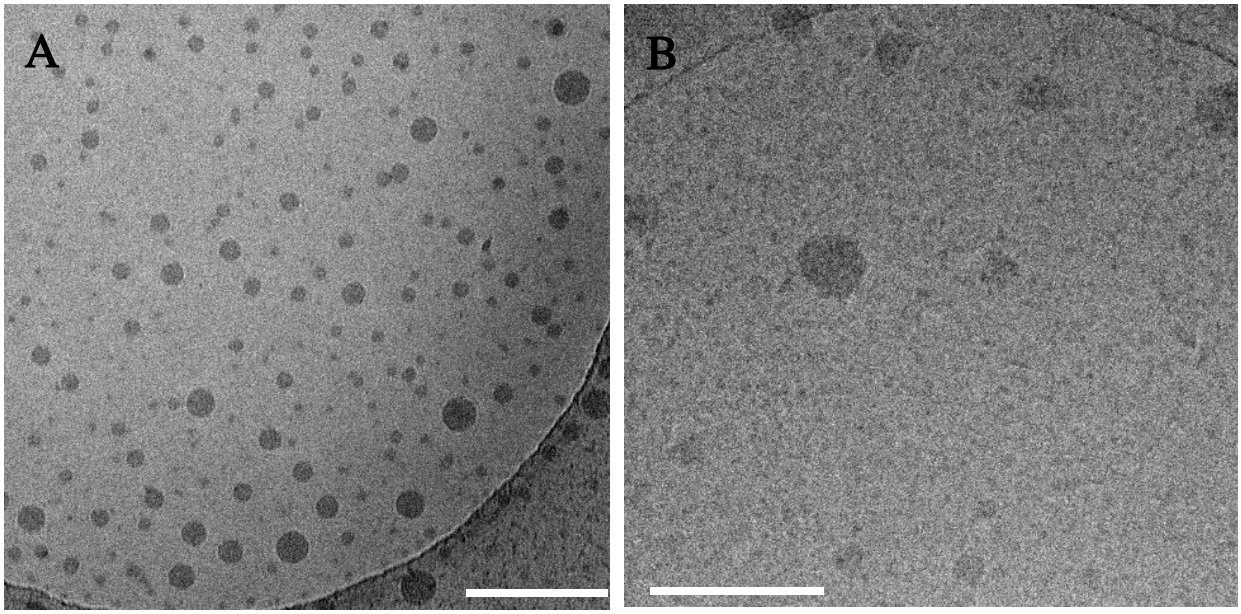

Figure 5. Cryo-TEM image of nanocarriers encapsulating A) VitEAc and B) OVA with 100% TNP surface coverage. Scale bar = 200 nm.

In vivo coadministration of nanocarriers and free OVA protein

To evaluate the role of hapten presentation on the surface of nanocarriers, nanocarriers with VitEAc in the core were co-administered with free OVA *in vivo*. Day 28 ELISA results are presented in Figure 6. Anti-TNP IgG was detected for all cases in which TNP was presented on NC surfaces, demonstrating the ability of the FNP NCs as hapten carriers for the induction of

View Article Online
DOI: 10.1039/D6PM00082G

hapten-specific antibodies. In terms of the effect of surface coverage, these results suggest that higher levels of haptenation on an individual NC yielded a higher titer of hapten-specific antibodies. The NCs with 100% of surface polymers terminated in TNP (group 4 in Figure 6) induced an anti-TNP IgG concentration approximately 10-fold higher than the NCs with 10% of surface polymers terminated in TNP (group 2 in Figure 6). As the total mass of TNP presented on NC surfaces was fixed between the two groups (groups 2 and 4 in Figure 6), the higher surface coverage with TNP may be responsible for this difference. The formulations containing 10% surface TNP coverage exhibited greater inter-animal variability and less consistent antibody responses compared to the 100% TNP surface coverage formulation. In contrast, nanocarriers with 100% TNP surface coverage produced more potent and reproducible anti-TNP IgG responses despite a lower total nanoparticle dose, suggesting that high hapten surface density may be an important factor for robust B-cell activation and consistent immunogenicity.

An additional experiment was performed in which the NC formulation with 10% of polymer surface chains terminated in TNP was dosed at one-tenth the dose as the other tests in this series (i.e. 0.06 ug total surface TNP per dose, compared to 0.6 ug total surface TNP per dose). Interestingly, the concentration of anti-TNP IgG induced by day 28 was similar in both cases. This is an unexpected result and indicates that effective B-cell activation may be also a function of hapten surface density above a threshold level of surface-presented hapten. The obtained results warrant future examination in a comprehensive dose-response test series.

View Article Online
DOI: 10.1039/D6PM00082G

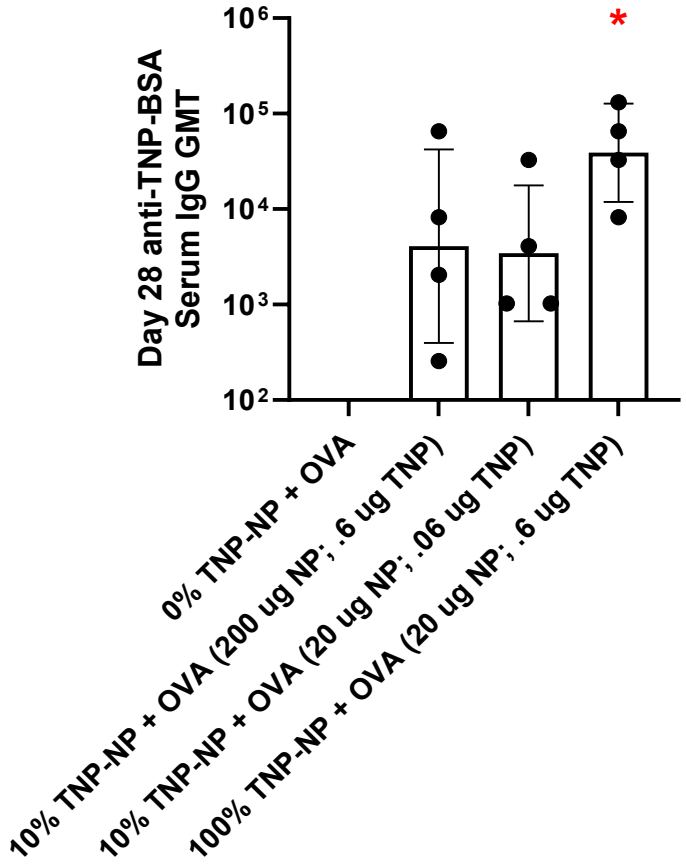

Figure 6. Anti-TNP IgG 28 days after dosing. Mice were vaccinated by the intramuscular route on days 0 and 14 with different TNP-NP formulations that include different concentrations of TNP on their surface and free soluble ovalbumin as an antigen to provide T cell help. On Day 28, blood was collected, and serum tested for the presence of anti-TNP IgG by ELISA. Kruskal-Wallis nonparametric test with Dunn's multiple comparison post-test was used to determine statistical differences in anti-TNP serum IgG compared to 0% TNP-NP. The overall p-value = 0.003. The adjuvanted p-value comparing each immunization group to 0% TNP-NP + OVA is as follows: 10% TNP-NP + OVA (200 μg NP; .6 μg TNP; p = 0.373), 10% TNP-NP + OVA (20 μg NP; .06

View Article Online
DOI: 10.1039/D6PM00082G

μg TNP; p = 0.568), and 100% TNP-NP + OVA (20 μg NP; .6 μg TNP; p = 0.0334). *: $p < 0.05$

Results suggest that FNP NCs may be effective carriers for haptens.

In vivo administration of FNP nanocarriers encapsulating OVA protein

The immunogenicity of TNP-decorated FNP NCs containing OVA in the core was then assessed and compared against a commercially-available OVA-TNP conjugate vaccine. The OVA-TNP antigen consists of ovalbumin as a protein carrier molecule that is chemically conjugated to the TNP hapten. We expect mice immunized with the OVA-TNP antigen to develop antibodies that recognize OVA-TNP and validate that our immunization and ELISA techniques are effective, so these antibodies were monitored as an ELISA positive control. Utilizing the OVA-TNP antigen in ELISA assays allows detection of antibodies that recognize the TNP hapten and the OVA carrier protein but does not allow for measuring antibodies specific for OVA or TNP alone. Therefore, we also included unconjugated OVA and TNP-BSA as ELISA antigens to measure OVA-specific and TNP-specific antibodies, respectively. Utilizing unconjugated OVA as an ELISA antigen will ensure that we measure only antibodies that bind OVA without measuring antibodies that bind TNP. Likewise, the TNP-BSA conjugate antigen allows us to measure only TNP-specific antibodies without antibodies that recognize OVA. The TNP-BSA antigen is another TNP-conjugate antigen that combines the bovine serum albumin protein with TNP. The mice in this experiment were immunized with vaccines containing TNP but not BSA. Therefore, the resulting antibody response detected using the TNP-BSA antigen ensures that we are solely measuring the response to TNP. 10 μg of MPL (a common standard adjuvant used clinically to stimulate immune

View Article Online
DOI: 10.1039/D6PM00082G

responses[33]) was used as an adjuvant in the animal studies here. The vaccine-induced antibody responses against OVA-TNP, unconjugated OVA, and TNP-BSA are listed below.

As reported in Figure 7, immunization with MPL-adjuvanted OVA-TNP protein conjugate vaccines induced elevated serum OVA-TNP- and TNP-specific IgG antibodies, but did not induce detectable OVA-specific IgG antibodies. The lack of OVA-specific antibodies observed in mice immunized with the OVA-TNP conjugate antigen may be a result of TNP serving as a carrier immunogenicity reducing hapten (CIRH) under the conditions of conjugation to the OVA protein, which occurs in some protein-hapten systems.[29] Mice immunized with 0% TNP and 1% TNP FNP NC vaccines developed serum OVA-TNP- and OVA-specific serum IgG responses but did not demonstrate detectable TNP-specific serum IgG responses. However, increasing the surface coverage of TNP to 10%, 50%, or 100% of surface polymer chains led to induction of elevated serum OVA-TNP-, OVA-, and TNP-specific IgG antibodies in mice that received two IM immunizations with the OVA-TNP NC conjugate vaccines. The magnitude of TNP-specific serum IgG observed in mice immunized with TNP NC containing 50 and 100% surface coverage was statistically similar to mice immunized with the OVA-TNP protein conjugate. OVA-TNP-specific serum IgG levels were comparable between all vaccine groups, and all mice immunized with NCs containing OVA developed detectable OVA-specific serum IgG responses. These results show that NCs with 100% TNP surface coverage induce significantly higher anti-TNP-BSA serum IgG titers than NCs with 10% coverage. This confirms that TNP-specific IgG levels are dependent on surface hapten density, consistent with the previous experiment. While similar TNP-BSA serum IgG titers were observed in mice immunized with the 50% and 100% TNP nanocarriers and the OVA-TNP conjugate, the systems differ in both total hapten dose and mode of presentation. The

View Article Online
DOI: 10.1039/D6PM00082G

OVA-TNP conjugate delivers approximately 1.48 μg TNP per dose, whereas the 100% and 50% surface-functionalized nanocarriers contain ~0.63 and 0.315 μg TNP per dose, respectively. Despite this lower hapten dose, comparable TNP-specific IgG responses were observed, suggesting that hapten presentation on the nanocarrier surface is efficient and that immunogenicity is not solely governed by total hapten quantity. In addition, the nanocarrier platform offers key advantages, including tunable hapten density, modular formulation design, and scalable manufacturing via FNP.

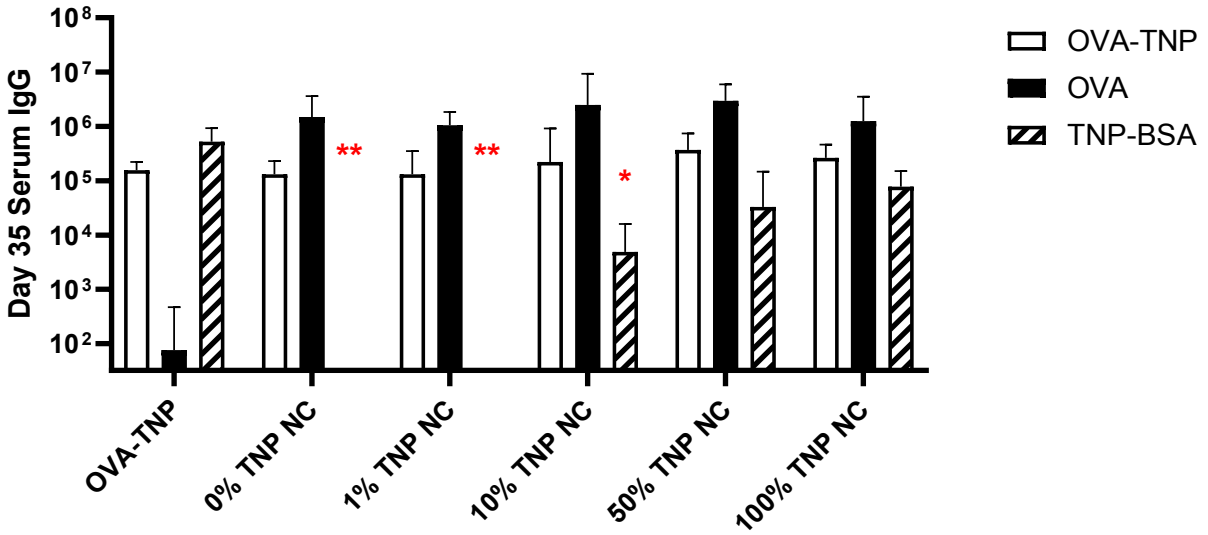

Figure 7. OVA-TNP NC vaccines induce potent OVA- and TNP-specific antibody responses. Female BALB/c mice received two IM immunizations with MPL-adjuvanted OVA-TNP protein conjugated vaccines or MPL-adjuvanted OVA-encapsulated FNP-prepared NCs with various densities of TNP surface coverage. Serum collected on Day 35 was measured for OVA-TNP-, TNP-, and OVA-specific IgG by ELISA. A nonparametric Kruskal-Wallis test with the Dunn's

View Article Online
DOI: 10.1039/D6PM00082G

multiple comparison post-test was used to compare vaccine-induced antigen-specific serum IgG responses to mice immunized with OVA-TNP protein conjugate. Statistical comparisons for all groups were performed relative to the OVA-TNP protein conjugate control group. **: $p < 0.01$, *: $p < 0.05$.

CONCLUSION

These results demonstrate proof of principle that polymeric NCs formed by FNP may be a suitable platform technology for formulating carriers for small molecule haptens to induce the formation of hapten-specific antibodies. Many small molecule hapten candidates can be rapidly conjugated to the end of commercially-available PCL-*b*-PEG-R polymers terminated with -NH_2, -COOH, -SH, or other functional groups, and the polymers subsequently used in FNP to create hapten-decorated NCs.

The results here also suggest that encapsulating the T-helper antigenic protein may not be necessary. The anti-TNP IgG induced by NCs with 100% of polymer surface chains terminated in TNP in the first (co-administration with free soluble OVA) and second (co-administration with encapsulated OVA) tests were comparable. The degree of surface haptenation does appear to be a factor in anti-TNP antibody induction, however. In both experiments, a higher degree of surface polymer chains terminated with the hapten elicited a higher titer of anti-TNP IgG.

The FNP NCs tested here did not outperform the commercially-available OVA-TNP conjugate antigen, and did elicit an OVA-specific IgG in addition to a TNP-specific IgG, where the commercially-available OVA-TNP conjugate only induced the desired TNP-specific IgG. Although pre-existing carrier-specific immunity may be a factor that reduces the immunogenicity to the hapten, elevated hapten density, multiple booster immunizations, or high vaccine doses may

View Article Online
DOI: 10.1039/D6PM00082G

be mechanisms to circumvent carrier-induced epitopic suppression[34]. Importantly, because the nanocarrier platform does not rely on covalent linkage between hapten and carrier, antigen and hapten components can be independently varied, providing a potential route to mitigate carrier-related effects through formulation design.

This initial study illustrates proof of concept, and additional work will be needed to establish the full design space and completely evaluate efficacy for this approach. Here, immune responses were evaluated primarily based on antibody titers without assessment of their functional activity or affinity, which will be the subject of future work. Likewise, the long-term durability and the impact of repeated boosting should be examined, as well as a comprehensive dose-response analysis across different hapten densities. Future studies should therefore focus on the biological activity of the induced antibodies, rather than titer alone. For example, if the NC-induced hapten-specific IgG binds more effectively to and neutralizes its target than the IgG induced by the protein-hapten conjugate (which we hypothesize may be the case, given the higher level of hapten coverage per surface area on the NC compared to the protein-hapten conjugate, and the physical separation between hapten and antigen by the 5kDa PEG chains), this could justify the lower antibody titer. The NC approach should also be more rapidly generalizable than the protein-hapten conjugate approach, which depends more strongly on the chemistry of the specific hapten and protein (and, for example, the commercially-available OVA-TNP conjugate product had been discontinued at the time of this writing). The NC approach also allows for the possibility of e.g. encapsulating adjuvants for co-localization, which merits further exploration. Future studies will optimize vaccine conditions (hapten dose, density, specific carrier, adjuvants, long-term durability, and memory response) with haptens that contain biological activity to utilize functional assays that monitor vaccine-induced immunity.

View Article Online
DOI: 10.1039/D6PM00082G

ANIMAL WORK

All studies performed in animals were approved by the Duke University Institutional Animal Care and Use Committee under protocol #A253-23-12

CONFLICTS OF INTEREST

K.R., M.B., B. J.-W., and H.S. are named inventors on a provisional patent application related to this work.

ACKNOWLEDGEMENT

The authors acknowledge and thank Samuel Hartzler and Dr. Lauren Ann Metskas for their assistance obtaining preliminary cryo-TEM visualizations of one of the formulations presented here.

Some figures in this work were created using BioRender.com.

View Article Online
DOI: 10.1039/D6PM00082G

REFERENCES

1. Britch, S. C. & Walsh, S. L. Treatment of opioid overdose: current approaches and recent advances. *Psychopharmacol. 2022 2397* **239**, 2063–2081 (2022).
2. Martinez, S. *et al.* The potential role of opioid vaccines and monoclonal antibodies in the opioid overdose crisis. *Expert Opin. Investig. Drugs* **32**, 181–185 (2023).
3. Kosten, T. R. & Petrakis, I. L. The Hidden Epidemic of Opioid Overdoses During the Coronavirus Disease 2019 Pandemic. *JAMA Psychiatry* **78**, 585–586 (2021).
4. Dowell, D. *et al.* Treatment for Opioid Use Disorder: Population Estimates — United States, 2022. *MMWR. Morb. Mortal. Wkly. Rep.* **73**, 567–574 (2024).
5. Barr, G. A., Schmidt, H. D., Thakrar, A. P., Kranzler, H. R. & Liu, R. Revisiting dezocine for opioid use disorder: A narrative review of its potential abuse liability. *CNS Neurosci. Ther.* **30**, (2024).
6. Bell, J. & Strang, J. Medication Treatment of Opioid Use Disorder. *Biol. Psychiatry* **87**, 82–88 (2020).
7. Sofuoglu, M., Devito, E. E. & Carroll, K. M. Pharmacological and Behavioral Treatment of Opioid Use Disorder. *Psychiatr. Res. Clin. Pract.* **1**, 4–15 (2019).
8. Bloom, B. T. & Bushell, M. J. Vaccines against Drug Abuse—Are We There Yet? *Vaccines 2022, Vol. 10, Page 860* **10**, 860 (2022).
9. Sulima, A. *et al.* Design, Synthesis, and In Vivo Evaluation of C1-Linked 4,5-Epoxymorphinan Haptens for Heroin Vaccines. *Mol. 2022, Vol. 27, Page 1553* **27**, 1553 (2022).
10. Jalah, R. *et al.* Efficacy, but not antibody titer or affinity, of a heroin hapten conjugate vaccine correlates with increasing hapten densities on tetanus toxoid, but not on CRM197

View Article Online
DOI: 10.1039/D6PM00082G

carriers. *Bioconjug. Chem.* **26**, 1041 (2015).

11. Baruffaldi, F. *et al.* Preclinical Efficacy and Characterization of Candidate Vaccines for Treatment of Opioid Use Disorders Using Clinically Viable Carrier Proteins. *Mol. Pharm.* **15**, 4947–4962 (2018).
12. Stone, A. E. *et al.* Fentanyl conjugate vaccine by injected or mucosal delivery with dmLT or LTA1 adjuvants implicates IgA in protection from drug challenge. *npj Vaccines 2021 61* **6**, 1–11 (2021).
13. Pravetoni, M. & Comer, S. D. Development of vaccines to treat opioid use disorders and reduce incidence of overdose. *Neuropharmacology* **158**, 107662 (2019).
14. Kosten, T. R. Vaccines as Immunotherapies for Substance Use Disorders. *Am. J. Psychiatry* **181**, 362–371 (2024).
15. Barrientos, R. C. *et al.* Novel Vaccine That Blunts Fentanyl Effects and Sequesters Ultrapotent Fentanyl Analogues. *Mol. Pharm.* **17**, 3447–3460 (2020).
16. Crouse, B. *et al.* Mechanisms of interleukin 4 mediated increase in efficacy of vaccines against opioid use disorders. *npj Vaccines 2020 51* **5**, 1–13 (2020).
17. Laudenbach, M. *et al.* The Frequency of Naive and Early-Activated Hapten-Specific B Cell Subsets Dictates the Efficacy of a Therapeutic Vaccine against Prescription Opioid Abuse. *J. Immunol.* **194**, 5926–5936 (2015).
18. Liu, Y. H. *et al.* Hapten design and indirect competitive immunoassay for parathion determination: Correlation with molecular modeling and principal component analysis. *Anal. Chim. Acta* **591**, 173–182 (2007).
19. Hu, Y., Zhao, Z., Ehrich, M. & Zhang, C. Formulation of Nanovaccines toward an Extended Immunity against Nicotine. *ACS Appl. Mater. Interfaces* **13**, 27972–27982 (2021).

View Article Online
DOI: 10.1039/D6PM00082G

20. McCluskie, M. J. *et al.* Anti-nicotine vaccines: Comparison of adjuvanted CRM197 and Qb-VLP conjugate formulations for immunogenicity and function in non-human primates. *Int. Immunopharmacol.* **29**, 663–671 (2015).

21. McCluskie, M. J. *et al.* The effect of preexisting anti-carrier immunity on subsequent responses to CRM197 or Qb-VLP conjugate vaccines. *Immunopharmacol. Immunotoxicol.* **38**, 184–196 (2016).

22. Kumar, V., Wang, L., Riebe, M., Tung, H. H. & Prud'homme, R. K. Formulation and stability of itraconazole and odanacatib nanoparticles: Governing physical parameters. *Mol. Pharm.* **6**, 1118–1124 (2009).

23. Pagels, R. F., Edelstein, J., Tang, C. & Prud'homme, R. K. Controlling and Predicting Nanoparticle Formation by Block Copolymer Directed Rapid Precipitations. *Nano Lett.* **18**, 1139–1144 (2018).

24. Johnson, B. K. & Prud'homme, R. K. Flash NanoPrecipitation of Organic Actives and Block Copolymers using a Confined Impinging Jets Mixer. *Aust. J. Chem.* **56**, 1021–1024 (2003).

25. Markwalter, C. E., Pagels, R. F., Wilson, B. K., Ristroph, K. D. & Prud'homme, R. K. Flash NanoPrecipitation for the Encapsulation of Hydrophobic and Hydrophilic Compounds in Polymeric Nanoparticles. *JoVE (Journal Vis. Exp.* **2019**, e58757 (2019).

26. Tominaga, J., Kamiya, N. & Goto, M. An Enzyme-Labeled Protein Polymer Bearing Pendent Haptens. *Bioconjug. Chem.* **18**, 860–865 (2007).

27. Lipford, G. B., Hoffman, M., Wagner, H. & Heeg, K. Primary in vivo responses to ovalbumin. Probing the predictive value of the Kb binding motif. *J. Immunol.* **150**, 1212–1222 (1993).

View Article Online
DOI: 10.1039/D6PM00082G

28. NAKAJIMA-ADACHI, H. *et al.* Two Distinct Epitopes on the Ovalbumin 323-339 Peptide Differentiating CD4+T Cells into the Th2 or Th1 Phenotype. *Biosci. Biotechnol. Biochem.* **76**, 1979–1981 (2012).

29. Ristroph, K. D., Rummaneethorn, P., Johnson-Weaver, B., Staats, H. & Prud'homme, R. K. Highly-loaded protein nanocarriers prepared by Flash NanoPrecipitation with hydrophobic ion pairing. *Int. J. Pharm.* **601**, 120397 (2021).

30. Liu, Y. & Fox, R. O. CFD predictions for chemical processing in a confined impinging-jets reactor. *AIChE J.* **52**, 731–744 (2006).

31. Han, J. *et al.* A simple confined impingement jets mixer for flash nanoprecipitation. *J. Pharm. Sci.* **101**, 4018–4023 (2012).

32. Subraveti, S. N., Wilson, B. K., Bizmark, N., Liu, J. & Prud'homme, R. K. Synthesizing Lipid Nanoparticles by Turbulent Flow in Confined Impinging Jet Mixers. *J. Vis. Exp.* **2024-August**, e67047 (2024).

33. Baldrick, P., Richardson, D., Elliott, G. & Wheeler, A. W. Safety Evaluation of Monophosphoryl Lipid A (MPL): An Immunostimulatory Adjuvant. *Regul. Toxicol. Pharmacol.* **35**, 398–413 (2002).

34. Jegerlehner, A. *et al.* Carrier induced epitopic suppression of antibody responses induced by virus-like particles is a dynamic phenomenon caused by carrier-specific antibodies. *Vaccine* **28**, 5503–5512 (2010).

View Article Online
DOI: 10.1039/D6PM00082G

All data used in this study are shown as plotted in Figures 2, 3, 4, 6, and 7, or the micrographs in Figure 5. These are readily available upon reasonable request.